Presented at the 38th NWA Annual Meeting, Charleston, SC, October 12-17, 2013

NEARSHORE WAVE PREDICTION SYSTEM: ENHANCING MARINE FORECASTING CAPABILITIES DURING HIGH IMPACT EVENTS

Alex Gibbs
Alex.Gibbs@noaa.gov
NOAA/NWS/WFO Miami
Miami, FL

Pablo Santos
Pablo.Santos@noaa.gov
NOAA/NWS/WFO Miami
Miami, FL

André van der Westhuysen
Andre.VanderWesthuysen@noaa.gov
IMSG at NOAA/NWS/NCEP/EMC/MMAB
College Park, MD

Roberto Padilla
Roberto.Padilla@noaa.gov
IMSG at NOAA/NWS/NCEP/EMC/MMAB
College Park, MD

1. INTRODUCTION

The demand for high-resolution forecasts of coastal processes, including wind, water levels, currents and waves has been steadily increasing over the past decade. The global operational multi-grid WAVEWATCH III® wave model (WW3, Tolman et al. 2002; Chawla et al. 2013), run by the National Weather Service's (NWS) National Centers for Environmental Prediction (NCEP), features a grid resolution of up to 4 arc-min (≈7.5 km) in these coastal regions, which does not provide sufficient forecaster guidance. Centralized modeling at NCEP at these nearshore scales is impractical from a computational point of view. In addition, regions differ with respect to the relevant physical processes, resolution requirements, and so on. It is therefore desirable that forecasters at local Weather Forecast Offices (WFOs) have control over the local model setup, and produce wave forecasts that are consistent with their local wind forecasts. For these reasons, the NWS is following an approach of decentralized nearshore wave computation. The Advanced Weather Interactive Processing System (AWIPS) is an information processing, display, and telecommunications system that is the cornerstone of the NWS's operational forecasting infrastructure at WFOs and National Centers such as the National Hurricane Center (NHC) and the Ocean Prediction Center (OPC). The NWS is currently in the process of upgrading to the more advanced AWIPS II, offering the opportunity to integrate local model guidance systems, such as high-resolution wave and surge models.

The aim of this work is to develop a real-time, deterministic modeling system, run locally at WFOs, which would provide high-resolution, wave model guidance to forecasters, and which would be fully integrated into AWIPS II. The resulting system is called the Nearshore Wave Prediction System (hereafter NWPS). It is intended to consolidate and extend the earlier successful pilot systems IFP-SWAN (Willis et al. 2010) and SR-SWAN (Settelmaier et al. 2011).

The NWPS provides high-resolution wave model guidance over a given WFO or National Center's marine domain of responsibility. The wave model SWAN (Booij et al. 1999), or a nearshore version of WW3 (Tolman et al. 2002), is applied as the underlying nearshore wave model, with boundary conditions and forcing being provided by a number of NOAA modeling systems. Within the WFO domain, the model is forced by forecaster-developed local wind fields from the Graphical Forecast Editor (GFE) inside of AWIPS II.

Details of these design elements and input sources are given in Section 2. The system is being calibrated and validated for a number of tropical and extra-tropical storms in the U.S. coast. Section 3 presents an example validation case for Hurricane Isaac (2012). Section 4 discusses additional development efforts and other potential applications. Section 5 closes the paper with conclusions.

2. METHOD

2.1 *System architecture*

Figure 1 shows the architecture and data flow of the NWPS system within the AWIPS II framework. Shown are the main structural components of AWIPS II, namely the EDEX data server and the CAVE data visualization and editing interface, and the NWPS computational unit. The block around these elements represents the AWIPS II Wide Area Network (WAN). The process begins with the forecaster preparing a series of official forecast wind fields in CAVE/GFE, and storing these in the EDEX data server. These wind fields are subsequently ingested into the NWPS computational unit. In addition, a number of model or observational data sets are used as input. These are either present in the AWIPS II WAN, or are ingested from NCEP's production ftp server via FTP/Local Data Manager (LDM) on the Local Data Acquisition and

Dissemination (LDAD) system. Once the forecaster wind fields and supplementary model inputs have been received, the wave model is initiated. The NWPS provides two core wave model options, namely SWAN and WW3. In the future, the ADvanced CIRCulation (ADCIRC) unstructured grid, finite element hydrodynamic model (Luettich et al. 1992; Luettich and Westerink 2004) will be included in the system to: further refine harmonic tidal cycles, resolve tidal currents within estuarine systems and to provide more accurate water levels and waves during surge events along vulnerable sections of the coast (see Section 5).

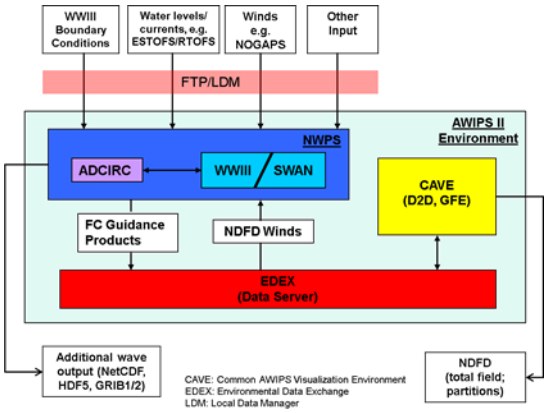

Figure 1: Architecture of the Nearshore Wave Prediction System within the AWIPS II environment.

Once the model run is complete, the output is sent to the EDEX data server for storage. The forecaster subsequently extracts these nearshore wave model guidance products and views them in CAVE/GFE. These are used to produce nearshore wave forecasts, which are posted to the National Digital Forecast Database (NDFD).

NWPS represents the first numerical model to reside inside of AWIPS II, and therefore presents unique challenges to this framework. The primary design is for NWPS to reside inside of the AWIPS II WAN, and to physically run the numerical model simulations on a 64-bit PX machine in the AWIPS II server rack. However, to accommodate more demanding numerical computations, a second design option is being supported, in which the numerical computation can be carried out on a separate workstation or cluster, physically residing outside of the AWIPS II WAN, and interfacing with AWIPS via the LDAD system. This is the option being used during alpha and beta testing prior to national deployment, and will continue to be supported afterwards. In addition, cloud computing options are being considered.

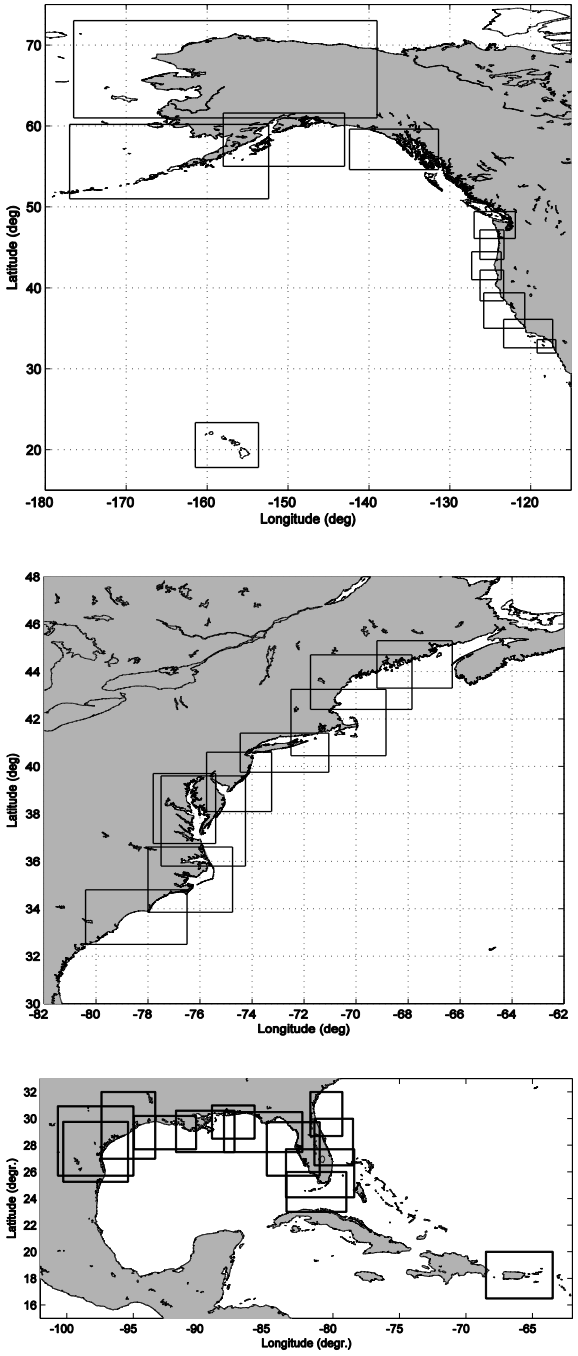

Figure 2. High-resolution NWPS model domains for coastal WFOs in the Western, Alaskan and Pacific Regions (top, WFO Guam not shown), Eastern Region (center) and Southern Region, including Puerto Rico and the Virgin Islands (bottom).

2.2 *Model grids and boundary conditions*

NCEP's global multi-grid wave watch model (hereafter WW3) computes wave fields over the globe on a 0.5 degree grid, with a series of nested regular grids that increase the resolution to 4-10 arc-min in coastal regions (Chawla et al. 2013). Two instances of WW3 are run, namely a non-tropical version that is forced with the Global Forecast System (GFS) atmospheric model (WW3 Multi-1 run) and a tropical cyclone version that is forced with a blend of NOAA Geophysical Fluid Dynamics Laboratory's (GFDL) cyclone atmospheric model and a background GFS field (WW3 Multi-2 run). Four cycles are produced daily (00Z, 06Z, 12Z and 18Z), each out to 192 hours. The WW3 results on the 4-10 arc-min coastal shelf grids that provide the boundary conditions to a series of high-resolution nested grids (one for each coastal WFO) along the contiguous United States coastline, Alaska, and island regions, which comprises the NWPS system (Figure 2). In addition, domains have been defined for the national centers NHC/TAFB and OPC (Figure 3).

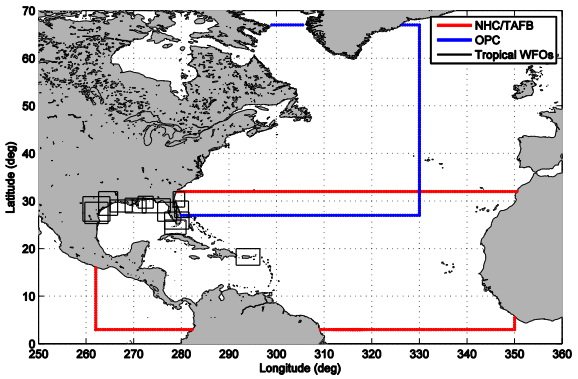

Figure 3. Ocean basin scale domains for NCEP's National Hurricane Center/Tropical Analysis and Forecast Branch (NHC/TAFB) and Ocean Prediction Center (OPC). Also shown are NWS's Southern Region WFOs, for which NHC/TAFB is to provide wave boundary conditions mainly during tropical cyclones. Eventually OPC would do the same for offices up the east coast.

Two operating modes of NWPS are distinguished: first, under extra-tropical conditions, all NWPS domains receive their wave boundary conditions directly from the WW3 Multi-1 (non-tropical). During tropical cyclone events, the official NHC wind forecast (Tropical Cyclone Message, or TCM) can differ strongly from the GFDL-GFS results, potentially rendering the WW3 Multi-2 boundary conditions inconsistent. Therefore, NHC/TAFB will run an instance of NWPS on their Atlantic model grid forced with the TCM wind fields, and provide the wave boundary conditions to the tropical NWPS grids within their domain (Figure 3). A similar approach is being considered for OPC and offices up the east coast outside the NHC/TAFB domain. The baseline computational grid setup of NWPS is a regular grid with a 1 arc-min resolution at each WFO, and an 18 km resolution over the larger NHC/TABF and OPC domains.

These computational grids at the WFOs are denoted as the primary or CG1 grids. Where required, WFOs can implement further sequential nested grids (CG2, CG3, etc.) to achieve higher resolutions over limited-area domains where more detail is required. For some WFOs, the wide range in spatial scales over their domains makes the application of unstructured grids more practical. An unstructured version of NWPS is being tested for the Florida Keys and is intended to be expanded further to other locations, such as: Puerto Rico, Hawaii, Alaska and New Orleans.

2.3 *Input sources*

Bathymetric and topography input to the NWPS are taken from various digital elevation models (DEMs) composed by the National Geophysical Data Center (NGDC). The baseline bathymetric data for the CG1 computational grids is provided by NGDC's 1 arc-min ETOPO1 Global Relief Model (Amante and Eakins 2009). This global data set provides coverage over all U.S. domains, with a vertical accuracy of ≈10 m, which is considered adequate offshore of the surf zone. ETOPO1 is also the source for bathymetric data applied in the WW3 model, ensuring consistency.

On a regional scale, NGDC's 3 arc-second Coastal Relief Model provides coverage of the contiguous U.S. coastal zone, Puerto Rico, and Hawaii. The 24 arc-second Coastal Relief Model for Southern Alaska (Lim et al. 2011) provides coverage of the Bering Sea, Aleutian Islands and Gulf of Alaska. The vertical accuracy of these models is estimated at ≈1 m. These sources of more detailed data are used to provide bathymetric data to the higher-resolution CG2, CG3, etc. nested computational grids in NWPS.

In the present version of NWPS, the influence of the water level and currents on the wave field is considered only in terms of one-way coupling. The often significant influence of the waves on water levels and coastal currents will be incorporated in future versions through local two-way coupling. Large-scale circulation currents such as the Gulf Stream can have a significant impact on coastal wave fields (e.g.

Haus 2007; Zhang et al. 2009). The effect of ocean currents are taken into account in NWPS by including surface current fields from NCEP's Global Real-Time Ocean Forecast System (RTOFS-Global, Mehra et al. 2011). RTOFS-Global is based on a $1/12^{o}$ eddy-resolving 3D baroclinic implementation of the HYbrid Coordinates Ocean Model (HYCOM, Chassignet et al. 2009), run once daily at NCEP.

In shallow coastal areas, good estimates of total water depths are important for accurate wave transformation. Water depths are determined by a combination of the topography-bathymetry and the contributions to the water level from tides and surge. Two modes of NWPS operation, related to the water level field source, are again distinguished.

First, tropical events characterized by high uncertainty in the atmospheric forcing. As a result, a probabilistic approach is followed by NHC to produce cyclone-related coastal surge forecasts during tropical cyclone events using the P-Surge system, based on the highly-efficient Sea, Lake, and Overland Surges from Hurricanes (SLOSH) model (Jelesnianski et al. 1992). One type of output from P-Surge is the composite surge level fields associated with a given exceedance level (e.g. 10-50%). Since these exceedance fields represent a single water level surface, they can be applied in a single deterministic NWPS run. Typically WFOs apply fields with low exceedance levels (e.g. 10%) far ahead of the time of landfall, and greater exceedances (e.g. 50%) close to landfall as the uncertainty decreases. Since SLOSH does not presently include tidal effects, external tidal fields have to be applied. For this, the (deterministic) tidal component of the Extratropical Surge and Tide Operational Forecast System (ESTOFS, Feyen et al. 2013) is used. ESTOFS is a 2D barotropic hydrodynamic model for the North Atlantic Ocean based on ADCIRC featuring both tidal and surge influences. Its tide component is combined with the P-Surge fields to obtain the final cyclone-related water level fields. Note, however, that P-Surge results will account for tide in the near future. Also, since the P-Surge fields include inundation of overland regions, it enables the computation of overland waves in flooded areas in NWPS, as will be shown in section 3.

During extra-tropical or non-tropical events, NWPS applies the deterministic output for total water level from ESTOFS. A similar approach to the one described here for tropical cases will be considered for extra tropical cases when a probabilistic version of ESTOFS is developed in the future to properly account for uncertainty.

2.4. *Wave model version and physics*

As mentioned above, NWPS offers SWAN and WW3 as core wave model options. The validation example presented here was produced using the SWAN model, version 40.81. The following settings for model physics are applied:

- Wind input and whitecapping according to Komen et al. (1984), as modified by Rogers et al. (2003).
- Quadruplet interactions using the DIA formulation by Hasselmann et al. (1985), with $C_{nl4} = 3x10^{7}$ and $\lambda = 0.25$.
- JONSWAP formulation of Hasselmann et al. (1973) for bottom friction with the coefficient $C_{f,JON} = 0.038\ m^2/s^3$.
- Depth-induced wave breaking according to Battjes and Janssen (1978), with $\alpha_{BJ} = 1.0$ and $\lambda_{BJ} = 0.73$.
- Triad interactions using the LTA formulation by Eldeberky (1996), with $\alpha_{EB} = 0.05$.

In addition, the following numerical settings were applied:

- Gibbs et al. (2012) studied time stepping and iteration options for SWAN, from which a time step of 600s combined with 1 iteration was selected as an optimal balance between accuracy and computational speed.

2.5 *Post-processing*

The high-resolution nearshore wave output from NWPS is post-processed into a number of model guidance products, including integral wave fields, wave spectra, and partitioned wave data. These are described below.

a) Integral wave fields wave spectra

The basic model output from NWPS are fields of the integral parameters significant wave height, peak wave period, and peak direction, typically produced every 3 h out to 102-120 h. In addition, frequency spectra are output at select locations. These outputs are all available for viewing and editing in the AWIPS II CAVE/GFE visualization module, from where it is posted to the NDFD.

b) Partitioned wave fields and time series

In order to provide forecasters with a comprehensive overview of the wave systems in their region of responsibility, the directional wave spectrum at each

grid point is partitioned using the inverse catchment method of Vincent and Soille (1991) and Hanson and Phillips (2001). With this method, various coherent regions of variance density in the directional spectrum are identified as separate partitions.

To ensure spatial and temporal coherence, these partitioning results are consolidated into wave systems by means of spatial and temporal tracking algorithms (Van der Westhuysen et al. 2013). The resulting wave systems are presented in terms of spatial fields and Gerling-Hanson time series plots. The latter show the progression of the wave height, period and direction of the various wave systems in time, along with the variation of local wind.

3. VALIDATION

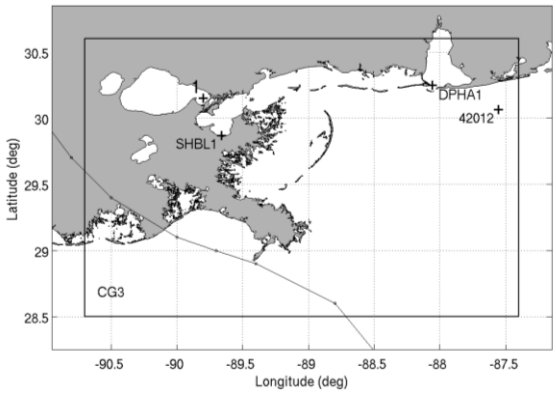

Figure 4. The 500 m inner nest New Orleans and Lake Pontchartrain domain residing within the NHC/TAFB Atlantic coarser 18 km grid. Included are the locations of stations DPHA1, SHBL1, NDBC 42012 and a sample point 1 over the eastern portion of Lake Pontchartrain. Line indicates best track of Hurricane Isaac.

To demonstrate the full functionality of the NWPS during a tropical cyclone event, a hindcast of Hurricane Isaac is discussed in the following sections. In this demonstration, Isaac was initially simulated over the NHC/TAFB domain (Figure 3) with a spatial resolution of 18 km, producing boundary conditions for a 1.86 km resolution nest over the WFO New Orleans/Baton Rouge domain, followed by a higher-resolution 500 m inner nest over New Orleans and Lake Pontchartrain (Figure 4), where Isaac made landfall.

Considering the limited wave observations over this nested domain during this event, aside from NDBC 42012, the primary focus of this hindcast is to illustrate the significant influence that increasing water

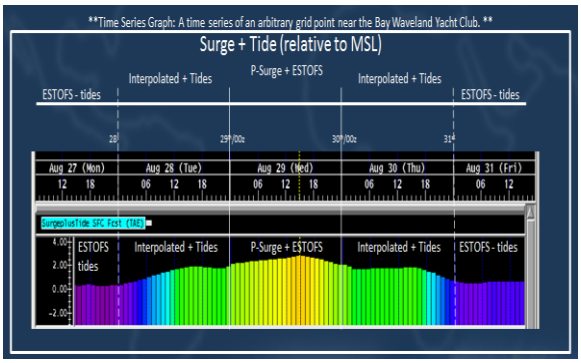

Figure 5. Time Series description of the interpolated water level (relative to MSL) input between the ESTOFS tidal component and the P-Surge guidance (20% exceedance height for this case).

levels due to surge has on the modeled wave fields over very shallow water regions.

3.1 *Model setup*

The bathymetry for the NHC/TAFB domain grid was taken from NGDC's 1 arc-min ETOPO1 model, whereas those for the WFO New Orleans/Baton Rouge domain and its high-resolution nest were compiled from NGDC's 1 arc-sec (≈30 meter) Northern Gulf Coast DEM. For this hindcast, atmospheric forcing was not taken from the usual TCM fields, but rather from reanalysis *H*Wind* fields (Powell et al. 1996), overlaid on background, 3-hourly, short-range forecast fields from GFS. The *H*Wind* fields represent the maximum sustained 1-min wind speeds over a sampling period of 5-10 min, denoted as $V_{60,600}$. These were converted to 10 min mean values (V_{600}), which are more appropriate for use in wind wave models. These quantities are related via a gust factor $G_{60,600}$, such that $V_{60,600} = G_{60,600}*V_{600}$ (Powell et al. 1996). Note that a similar conversion should be applied to TCM wind fields during forecast operations. A gust factor of $G_{60,600} = 1.05$ was selected based on a sampling period of 10 min and a "at sea" surface type (see Harper et al. 2010, Table 1.1). This composite wind field time series was produced for the period 22 Aug-31 Sept 2012, to capture the cyclone generation over the Atlantic.

For water levels, ESTOFS (tides)/P-Surge fields are applied as input to the wave model, as outlined in Section 2. Three runs are presented, each with a different treatment of the imposed water level fields: (i) an inundation run with P-Surge surge levels and ESTOFS tidal levels, in which the inundation of overland areas are included, (ii) a non-inundation

sensitivity run with P-Surge surge levels superimposed on ESTOFS tides, but with overland

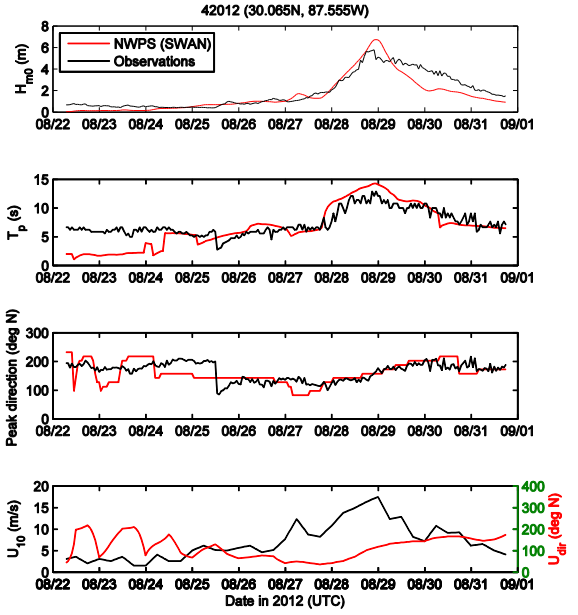

Figure 6. NWPS wave results at NDBC 42012, near Mobile, AL, showing hindcast significant wave height (H_{m0}), peak period (T_p) and peak directions against observations.

regions excluded (treated as dry points in the wave model), and (iii) a sensitivity run featuring only tides from ESTOFS (no surge component and no inundation). At present, the P-Surge water level fields are issued as spatially-varying, but stationary values, corresponding to the peak of the storm. Therefore, in order to obtain a realistic temporal variation, the water level field was interpolated from the ESTOFS meteorological tide input to this P-Surge level field (20% exceedance) on either side of the storm, as shown in Figure 5. In the future, time varying, incremental exceedance P-Surge fields will become available, avoiding the need for this interpolation procedure.

3.2 *Storm Overview and Results*

Although Isaac was a minimal category 1 hurricane prior to landfall (1200 UTC 28 August at 139 km or 75 nmi southeast of the Mississippi River), the combination of its slow forward movement toward the southeast Louisiana coast and large easterly wind field north of its track generated large waves and allowed an extensive amount of water to build up against the levees east of the Mississippi River. Estimated inundation (above ground level) calculated from USGS tide pressure sensors, USGS high-water marks, and NOS tide gauges in southeastern Louisiana ranged from 4-5 m (13-17 ft) at the peak of the surge (Berg 2013). Total significant wave heights

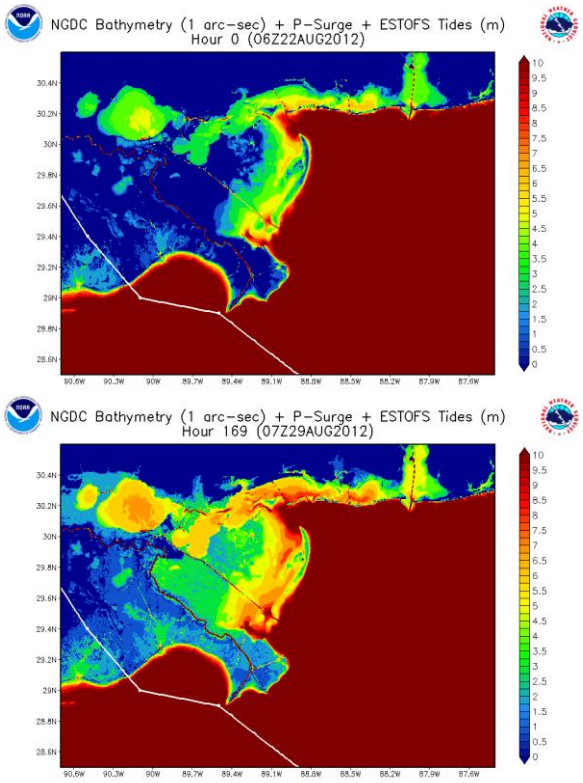

Figure 7. Field output from NWPS displaying the total water depth several days in advance of landfall (top) compared to the total water depth at or around landfall (bottom). Note the large inundation areas over the Mississippi Delta marshes and around Lake Pontchartrain. Hurricane best track included (white line).

of up to around 7 m were recorded at NDBC 42012, southeast of Mobile Bay (Figure 4). Figure 6 shows a time series of the modeled significant wave height, period and direction against observations. These all agree generally well during the second half of the run, as Isaac was approaching and making landfall.

a) Inundation test, including overland areas

Figure 7 shows the spatial distribution of the total water depths used in this model simulation several days leading up to the time of landfall (hr 0 of the simulation) versus the total water depths during the

peak of the surge (hr 169 of the simulation) at or around landfall. Peak inundation output from P-Surge

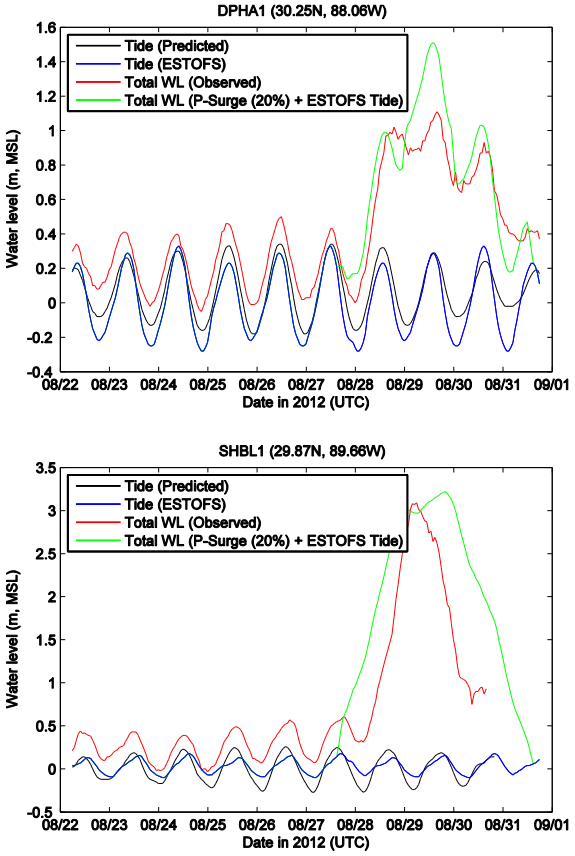

Figure 8. Observed and modeled water levels at two locations inside the high-resolution nest for WFO New Orleans/Baton Rouge: DPHA1 near Mobile, AL (top) and SHBL1 near New Orleans, LA (bottom).

(20% exceedance height) reached approximately 4 m between the Mississippi Delta and Lake Borgne, as Isaac was making landfall. Inundation between Lake Borgne and Pontchartrain ranged from 1.2-2.3 m (4-7.5 ft) just south of the Rigolets. These inundation levels are in close agreement with those reported by Berg (2013). Furthermore, water level rises due to surge over portions of the shallow Lake Maurepas, Pontchartrain and Borgne ranged from 1.5-2 times higher than the normal levels.

Figure 8 shows the time series of the ESTOFS/P-Surge water levels used in the model at the stations Dauphin Island (DPHA1) and Shell Beach (SHBL1), and compares them to observations. Although there are some differences between the total magnitudes and timing at and during the peak of the surge, the results generally agree well, with no conclusive positive or negative biases. It is worth mentioning that 20% exceedance heights are considered to be a safe

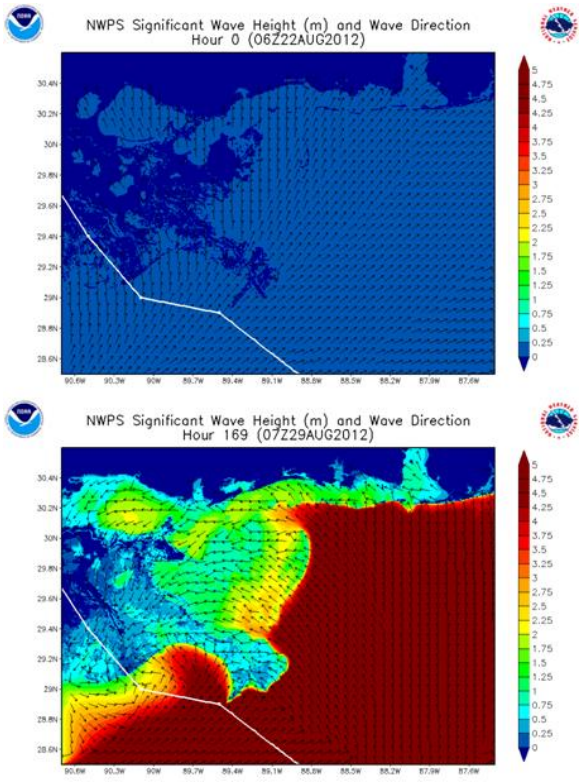

Figure 9. Field output from NWPS displaying the total significant wave height and peak wave direction several days in advance of landfall (top) compared to the total significant wave height and peak wave direction at or around landfall (bottom). Hurricane best track included (white line).

operational approach that speaks to potential heights that could reasonably be realized when factoring in uncertainty. So they are likely bound to be a high estimate of surge. Even so the results here generally agree well with observations albeit a bit on the hi side which is to be expected because of the low percentage based heights.

Figure 9 shows wave height and peak direction output from NWPS over the New Orleans and Lake Pontchartrain domain at hr 0 and at hr 169 (peak of the surge). Note the large areas of inundation over which wave energy is predicted.

Figure 10 shows a time series comparison of simulated wave heights at SHBL1 and over the very

shallow waters of the far eastern section of Lake Pontchartrain (point 1) for various water level inputs, suggesting large increases at the storm peak when considering the surge effect. One caveat noted in this inundation test is that we are not precisely resolving terrain during the wave computations, with regard to structures overland.

Therefore, wave results could contain a rather high bias downstream of flooded overland areas. Further testing will be necessary in this regard.

b) Non-Inundation test, excluding overland areas

Next, we investigate model results when inundated overland areas, alluded to above, are excluded (i.e. remain dry in the model). All wet grid points contain identical water levels as the first test. This test is important, since present nearshore wave and surge model systems (e.g. NWPS and ESTOFS (alpha version)) exclude overland regions. Figure 11 shows a spatial distribution of the total water levels used in this simulation, where only the sea points (grid points that are wet at MSL) were included. By excluding inundated land points, modeled wave heights over the wet grid points downstream of the previously flooded dry areas are notably different. The result in Figure 10 shows that significant wave heights at point 1 were reduced by up to 20% compared to the test run that included the inundated dry grids upstream of sample point 1, south of the Rigolets. At SHBL1, the difference in wave height is as much as 50%. This general pattern was consistent at other sample points just downstream of the previously flooded dry grid points. Including overland grid points therefore has a significant influence on both overland and sea points in the present case.

c) Tide-only sensitivity test

To demonstrate the full effects that surge can have on the model-estimated wave heights, the final test included only the tidal component from ESTOFS for the water level input. Figure 12 clearly shows a strong correlation between increasing water levels and higher simulated significant wave heights across shallow water regions of New Orleans, in this case. This shows that significant wave heights reached as high as two times the magnitude when surge was included. These significant differences are further illustrated in the wave height time series comparisons in Figure 10. Similar results were alluded to by Huang et al. (2010) across the Tampa Bay region, where an Ivan-like hurricane was simulated making landfall just north of Tampa Bay.

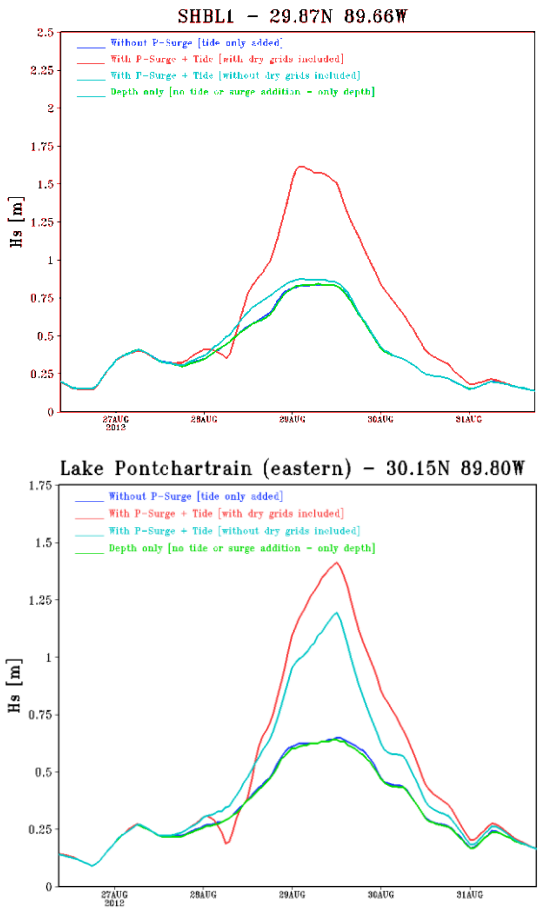

Figure 10. Time series of simulated significant wave height (H_S) at SHBL1 (top) and Lake Pontchartrain (point 1, bottom) for various input water levels.

4. ADDITIONAL DEVELOPMENT EFFORTS AND APPLICATIONS

The latest version of NWPS Alpha is currently running in all NWPS Southern Region offices, the Mid Atlantic coastal offices from Charleston to Wakefield, Gray and Caribou, Maine, Eureka, CA., and TAFB/NHC. As the project keeps moving forward toward implementation in every coastal office and AWIPS II, additional development and applications being worked on include: unstructured grids, wave climatologies, rip current forecasting, web interfaces, and ship route forecasts.

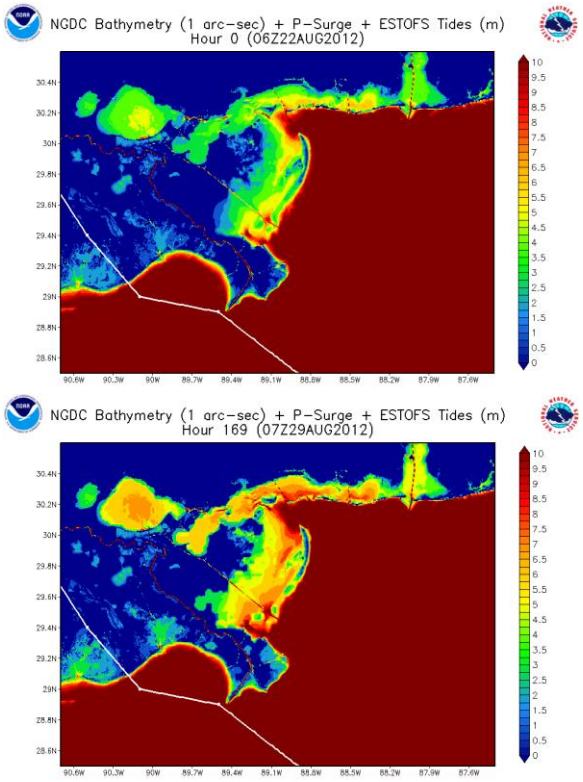

Figure 11. Same as Figure 7, except without dry grid points.

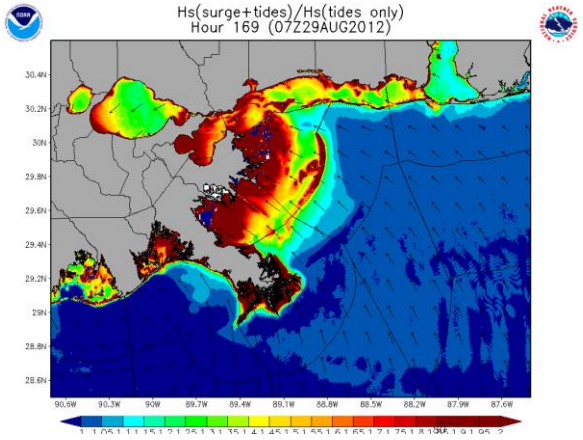

Figure 12. Field output from NWPS at Isaac's landfall, showing fractional increase of significant wave height due to the inclusion of the P-Surge surge levels (inundation zones omitted) relative to when only tide was factored in. Scale in the image ranges from 1-2 m (from blue to red).

4.1 *Unstructured Grids*

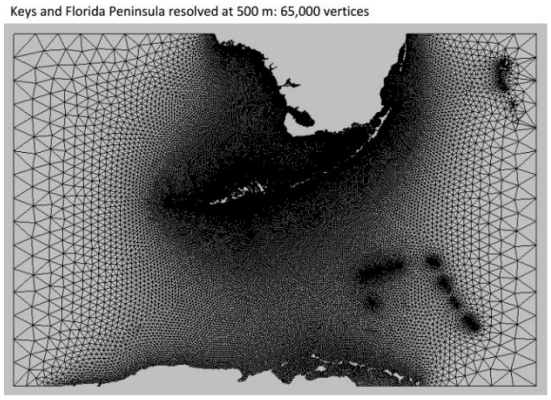

Figure 13. Unstructured grid for WFO Key West.

In order to resolve complex coastal areas, such as islands, consisting of large bathymetry gradients spatially, an unstructured version of NWPS is desired. The current structured version of the NWPS demands the development of high-resolution nesting using conventional regular grids to resolve these critical areas. This approach has its limitations due to large computational expenses that do not fit within the operational time constraints at a local forecast office. Therefore, an unstructured version of NWPS is being developed and will be included in future versions. This approach will provide realistic opportunities to resolve these complex regions concentrating necessary mesh resolutions in the areas of interest (i.e. inlets, bays and surf zone), while maintaining fewer grid points across the offshore zones where higher resolution is not desired. Figure 13 shows an example of an unstructured grid currently being developed and tested for the Key West Office within NWPS.

4.2 *Wave Climatologies*

One capability NWPS brings to coastal forecast offices is the development of wave climatologies across individual marine zones. Currently, a typical office running this model operationally typically produces two cycles per day. The grib2 data output from each run can be archived and aggregated for any time period over the years to generate synthetic model-based wave climatologies. This application was just started at WFO Miami in January of 2013. Figure 14 shows one sample case for the months of January and July of 2013 built for the Palm Beach County coastal waters based on the 24 hour model

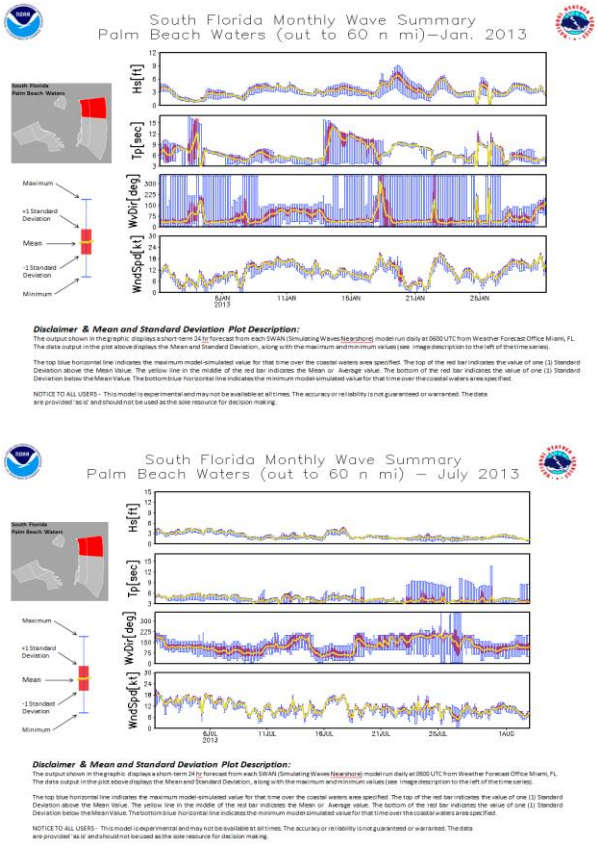

Figure 14. Wave Climatology for the Palm Beach Coastal Waters for the months of January (top) and July (bottom) of 2013. Climatologies are based on the 24 hours forecast from the 06Z daily runs at WFO Miami. Shown in the figure are significant waveheights (Hs), peak period (Tp), peak wave direction (WvDir), and wind speed (WndSpd).

forecasts. From a climatological stand-point, these graphics can be used to develop long-term climatological means as this effort is continued and built over a period of several years with means derived from multiple years of data. This example in Figure 14 illustrates a well-known case for the South Florida waters: a more active wave regime in the winter time versus summer due to stronger/weaker atmospheric forcing, respectively.

4.3 *Rip Current Forecasting*

The ability to generate high resolution wave output along critical bathymetry contours near the coast from NWPS has led to a valuable opportunity to merge the wave system with a rip current model recently developed by Dusek and Seim, 2013.

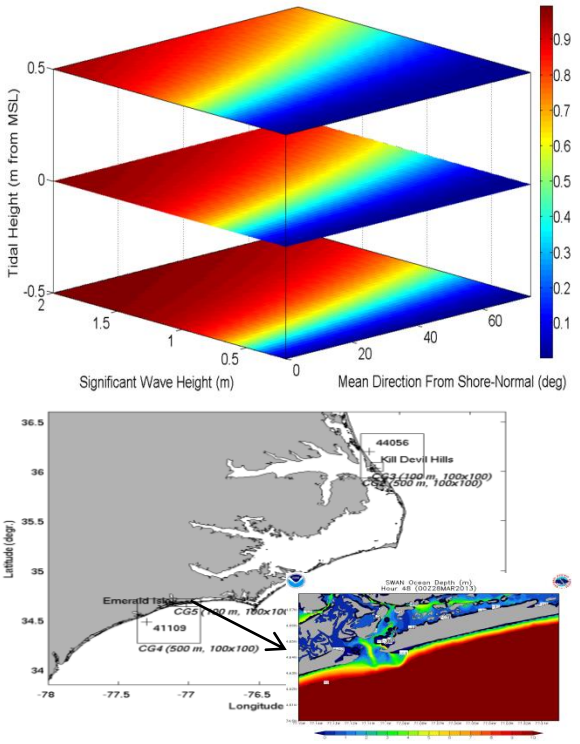

Figure 15. Rip Current Model + NWPS: developed to generate a statistical likelihood of hazardous rip currents at site MHX in Moorehead City, NC. High resolution output from the NWPS along bathymetry contours from the area of interest is provided as input to the rip current model.

A hindcast from May through September of 2013 was generated across the MHX (Moorehead City, NC) domain to output high resolution wave fields along the 5m bathymetry contour, which were provided as input to the rip current model developed.

NWPS fields provided along the 5m contour:

- NWPS Significant Wave Height
- NWPS Mean Wave Direction
- NWPS/ESTOFS Water level relative to MSL
- NWPS Hi-Res bathymetry

The rip current likelihood model (0 to 1) is shown in Figure 15. The lower the tide, the higher the significant wave height, and the closer the mean wave direction is to being perpendicular to the coast, the higher the likelihood of observing hazardous rip currents. In order to work properly, the calibration of the logistic regression model is region/site specific. Although it is being developed and validated

extensively for a couple of sites along the North Carolina coast, the model will soon be implemented and calibrated at WFO Miami for testing. We envision this capability extending elsewhere across coastal sites as a targeted application of the NWPS system.

4.4 *NWPS Web Interface*

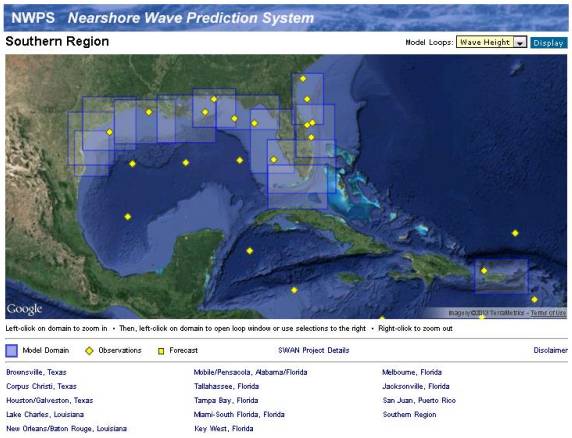

Figure 16. Web interface where users will be able to interactively access for any given office a variety of model output including significant wave heights, peak period, peak direction, 1-D spectral plots, Gerlin-Hanson plots, etc. The site under construction can be access at: http://innovation.srh.noaa.gov/nwps/swan-work.php.

NWS customers can also benefit from looking at the high resolution NWPS output on the web. A parallel project with NWPS is the development of a web interface (Figure 16) where users can access the following:

- Multi panel plots of significant wave height, peak period, peak direction, swell, currents, and water levels
- 1D spectral plots for select points
- Gerling Hanson plots plotting height, period, and direction of multiple wave systems.

While the interactive web interface is fully developed, real-time output plots of these parameters for NWS SR Coastal sites can also be accessed directly form the following site:

http://www.srh.noaa.gov/images/rtimages/xxx/nwps/
(replace xxx with office 3 letter ID, for example, WFO Miami would be mfl)

4.5 *Ship Route Forecast Program*

A recent addition being developed and included within NWPS will be the ability for coastal forecast offices to generate ship route forecasts featuring: a 2D graphic of NWPS parameter/s (i.e. Gulf Stream) with the ship track overlaid, times series of in-route total significant wave heights, dominant wave periods and peak wave directions. Figure 17 illustrates this concept applied across the Gulf Stream off of the South Florida coast from Lake Worth in Palm Beach County, FL to Bimini Island, Bahamas. Future additions could include wave steepness to compliment wave height and period, which would provide additional decision support to vessels supporting operational tasks that are highly restricted by critical wave thresholds and conditions.
The program is reasonably flexible and can be adapted by any coastal forecast site after inserting a set of defined locations to generate forecasts to and from within their respective limited area model.

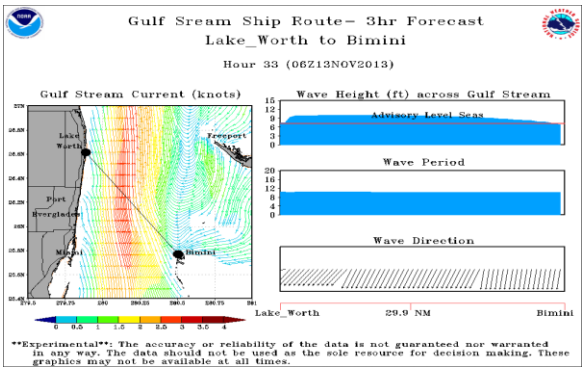

Figure 17. Ship route forecast from Lake Worth in South Florida to Bimini Island of the Bahamas across the Gulf Stream.

This program is unique due to the ability to plot cross-sectional time series plots along various track directions (i.e. 0-360 deg), whereas, the latest version of the GrADS plotting software included within NWPS only allows users to output cross-section forecasts with only one varying dimension, while keeping the other dimension constant (i.e. latitude or longitude). Future versions could include varying track directions that include several leg segments from the departure location to the final destination (i.e. Miami to Bimini to Port Everglades).

5. CONCLUSIONS

This paper presented the development of the Nearshore Wave Prediction System, a real-time, deterministic modeling system, which is being or will be run locally at every coastal Weather Forecast

Office, providing high-resolution, wave guidance to forecasters that incorporates one-way, currents, surge and tide coupling. The validation of the proposed system was shown for the field case of Hurricane Isaac (2012). Based on the results of this study, the following conclusions can be drawn:

- With NWPS, coastal Weather Forecast Offices nationwide will be able to produce detailed nearshore wave model guidance consistent with their local wind forecast.
- During tropical cyclone events, WFOs will be able to initialize their local wave model grid boundaries with the output of a coarser NHC/TAFB wave model run (forced by the official NHC wind forecast) and utilize the P-Surge forecast guidance (i.e. 10-50% exceedance heights) as water level input. This will lead to a seamless mosaic of digital marine forecasts between coastal WFOs impacted consistent with official forecasts.
- Increased water levels due to surge have an enormous impact on the computed total significant wave heights across shallow water regions, such as the domain of responsibility of WFO New Orleans/Baton Rouge.
- A higher density of overland wave observations is needed for further validation of the wave height sensitivity results presented here.

Last but not least, NWPS will expand the WFOs ability to enhance marine products and services including targeted applications for decision support services.

5. REFERENCES

Amante, C. and B. W. Eakins, 2009: ETOPO1 1 Arc-Minute Global 386 Relief Model: Procedures, Data Sources and Analysis. *NOAA Technical Memorandum* NESDIS NGDC-24, 19 pp.

Battjes, J. A. and J. P. F. M. Janssen, 1978: Energy loss and set-up due to breaking of random waves. *Proc. 16th Int. Conf. Coastal Eng*., ASCE, 569-587.

Berg, R., 2013: Tropical Cyclone Report Hurricane Isaac (AL092012) 21 August – 1 September 2012. *National Hurricane Center*. Retrieved on January 28, 2013, from www.nhc.noaa.gov/data/tcr/AL092012_Isaac.pdf

Booij, N., Ris, R.C., Holthuijsen, L.H., 1999: A third-generation wave model for coastal regions: 1. Model description and validation. *J. Geophys. Res*. 104 (C4), 7649-7666.

Chassignet, E.P., H.E. Hurlburt, E.J. Metzger, O.M. Smedstad, J. Cummings, G.R. Halliwell, R. Bleck, R. Baraille, A.J. Wallcraft, C. Lozano, H.L. Tolman, A. Srinivasan, S. Hankin, P. Cornillon, R. Weisberg, A. Barth, R. He, F. Werner, and J. Wilkin, 2009: U.S. GODAE: Global Ocean Prediction with the HYbrid Coordinate Ocean Model (HYCOM). *Oceanography*, 22(2), 64-75.

Chawla, A., Tolman H. L., Gerald, V., Spindler, D., Spindler, T., Alves J-H. G. M., Cao, D., Hanson J. L. and Devaliere E-M, 2013: A multi grid wave forecasting model: A new paradigm in operational wave forecasting, *Weather and Forecasting*, in press.

Dusek, G. and Seim, H., 2013. A probabilistic rip current forecast model. *Journal of Coastal Research*. 29(4), 909-925

Eldeberky, Y. (1996), Nonlinear transformations of wave spectra in the nearshore zone, PhD thesis, Fac. of Civ. Eng., Delft Univ. of Technol., Delft, Netherlands. 203 pp. http://repository.tudelft.nl

Feyen, J.C., Y. Funakoshi, A.J. van der Westhuysen, S. Earle, C. Caruso Magee, H.L. Tolman, F. Aikman III, 2013: Establishing a Community-Based Extratropical Storm Surge and Tide Model for NOAA's Operational Forecasts for the Atlantic and Gulf Coasts. *Proc. 93rd AMS Annual Meeting*, Austin, TX.

Gibbs, A, P. Santos, A.J. van der Westhuysen and R. Padilla, 2012: NWS Southern Region Numerical Optimization and Sensitivity Evaluation in Non-Stationary SWAN Simulations. *Proc. 92nd AMS Annual Meeting*, New Orleans, LA.

Hanson, J.L. and O.M. Phillips, 2001: Automated Analysis of Ocean Surface Directional Wave Spectra. *J. Atmos. and Ocean Tech*., 18, 277-293.

Huang, Y., R.H. Weisberg, and L. Zheng, 2010: Coupling of surge and waves for an Ivan-like hurricane impacting Tampa Bay, Florida region. *J. Geophys. Res*., 115, C12009.

Hasselmann, K., T. P. Barnett, E. Bouws, H. Carlson, D.E. Cartwright, K. Enke, J.A. Ewing, H. Gienapp, D.E. Hasselmann, P. Kruseman, A. Meerburg, P. Mueller, D.J. Olbers, K. Richter, W. Sell and H. Walden, 1973: Measurements of

wind-wave growth and swell decay during the Joint North Sea Wave Project (JONSWAP). *Ergaenzungsheft zur Deutschen Hydrographischen Zeitschrift*, Reihe A(8), 12, 95 pp.

Hasselmann, S. and K. Hasselmann, 1985: Computations and parameterizations of the nonlinear energy transfer in a gravity-wave spectrum, Part I: A new method for efficient computations of the exact nonlinear transfer integral. *J. Phys. Oceanogr*., 15, 1369-1377.

Haus, B.K., 2007: Surface current effects on the fetch-limited growth of wave energy, *J. Geophys. Res*., 112, C03003, doi:10.1029/2006JC003924.

Harper, B.A., J. D. Kepert J. D. Ginger, 2010: Guidelines for Converting Between Various Wind Averaging Periods in Tropical Cyclone Conditions. *World Meteorological Organization*. WMO/TD-No. 1555.

Jelesnianski, C.P., J. Chen, and W.A. Shaffer, 1992: SLOSH: Sea, lake, and overland surges from hurricanes. *NOAA Technical Report* NWS 48, National Oceanic and Atmospheric Administration, U. S. Department of Commerce, 71 pp.

Komen, G.J., S. Hasselmann and K. Hasselmann, 1984: On the existence of a fully-developed wind-sea spectrum. *J. of Phys. Oceanogr*. 14, 1271-1285.

Lim, E., B.W. Eakins, and R. Wigley, 2011: Coastal Relief Model of Southern Alaska: Procedures, Data Sources and Analysis, *NOAA Technical Memorandum* NESDIS NGDC-43, 22 pp.

Luettich, R.A. and J.J. Westerink, 2004: Formulation and Numerical Implementation of the 2D/3D ADCIRC Finite Element Model version 44.XX. http://adcirc.org/adcirc theory 2004 12 08.pdf.

Luettich, R.A., J.J. Westerink, and N.W. Scheffner, 1992: ADCIRC: An Advanced Three-Dimensional Circulation Model of Shelves, Coasts, and Estuaries, Report 1: theory and methodology of ADCIRC-2DDI and ADCIRC-3DL. *U.S. Department of the Army, Technical Report* DRP-92-6.

Mehra, A. I. Rivin, H.L. Tolman, T. Spindler and B. Balasubramaniyan, 2011: A Real Time Operational Global Ocean Forecast SyZhangstem (Poster). GODAE OceanView - GSOP - CLIVAR *Workshop on Observing System Evaluation and Intercomparisons*, Univ. of California Santa Cruz, CA, USA, 13-17 June.

Powell M.D., Houston, S.H., Reinhold, T.A., 1996: Hurricane Andrew's Landfall in South Florida. Part I: Standardizing Measurements for Documentation of Surface Wind Fields. *Weather and Forecasting*, 11, 304-328.

Rogers, W.E., P.A. Wang and D.W. Wang, 2003: Investigation of wave growth and decay in the SWAN model: Three regional scale applications. *J. Phys. Oceanogr.*, 33, 366-389.

Settelmaier, J. B., A. Gibbs, P. Santos, T. Freeman, D. Gaer, 2011: Simulating Waves Nearshore (SWAN) Modeling Efforts at the National Weather service (NWS) Southern Region (SR) Coastal Weather Forecast Offices (WFOs). *Proc. 91st AMS Annual Meeting*, Seattle, WA.

Tolman, H.L., B. Balasubramaniyan, L.D. Burroughs, D.V. Chalikov, Y.Y. Chao, H.S. Chen and V.M. Gerald, 2002: Development and implementation of wind generated ocean surface wave models at NCEP. *Weather and Forecasting*, 17, 311-333.

Van der Westhuysen, A.J, J.L. Hanson E.-M. Devaliere, 2013. Spatial and temporal tracking of wave fields from ocean basin scales to coastal waters. *J. Atmos. and Ocean Tech*., submitted.

Vincent, L. and P. Soille, 1991: Watersheds in digital spaces: An efficient algorithm based on immersion simulations. *IEEE Transactions of Pattern Analysis and Machine Intelligence*, 13, 583–598.

Willis, M. C., E.-M. Devaliere, J. Hanson, R. Hawkins, J. Lewitsky, D. King, T. Nicolini, S. Tjaden, C. Morgan, S. Schumann, M. Colby, and J. Elardo, 2010: Implementing the SWAN Wave Model at Three East Coast National Weather Service Offices. *Proc. 90th AMS Annual Meeting*, Atlanta, GA.

Zhang, F.W., M. William, B. Drennan, K. Haus, and H.C. Graber, 2009: On wind-wave-current interactions during the Shoaling Waves Experiment, *J. Geophys. Res*., 114, C01018, doi:10.1029/2008JC004998.

Acknowledgements. We would like to thank Arun Chawla and Mark Powell for useful discussions during the execution of this work.